



SEISMIC DEMANDS ON THREE-STORY SCBF SYSTEMS - COMPARISON OF FIBER-BASED MODEL AND FINITE ELEMENT-BASED MODEL

Chui-Hsin Chen¹, Yuli Huang² and Stephen Mahin³

ABSTRACT

Concentrically braced steel frames are expected to exhibit complex nonlinear behavior during strong earthquake ground shaking. To improve understanding of seismic behavior of steel braced frames and to help identify improved design and analysis procedures, an extensive program of analyses was carried out. The analytical studies of three-story SCBF buildings were conducted using fiber-based platform OpenSees and finite element software LS-DYNA. The case study of structural behavior shows that the OpenSees models with fatigue materials have larger story drifts once the braces fracture and lead to a larger residual interstory drift at the end of the time history. Due to the fracture of braces in OpenSees models with fatigue materials, the strength and stiffness are reduced after the fracture. LS-DYNA results show a more gradual change in strength before and after reaching the peak strength. Moreover, the ultimate failure modes may differ significantly for the two approaches. From a statistical perspective, the difference between OpenSees beam-element model and LS-DYNA shell-element model results is less than the dispersion for different ground motions by the same model. Therefore, the inelastic responses under consideration can be obtained from analysis using beam- or shell-element model, resulting in equally accurate statistical predictions of overall response quantities, like maximum story drift.

Introduction

As part of the NEES Small Group research project “Hybrid Simulation of Tomorrow’s Concentrically Braced Steel Frames,” a series of nonlinear dynamic analyses are being carried out. The goals of these analyses is to improve understanding of the behavior of conventionally and buckling restrained braced frames, devise appropriate loading protocols for experimental assessment of braced frames, and to identify improved performance-based design and analysis procedures. This research extends earlier work by Uriz and Mahin (2008) by considering a broader range of bracing configurations, building heights and earthquake motions, as well as by including more refined finite element models.

¹Graduate Student Researcher, Dept. of Civil and Environmental Engineering, UC, Berkeley, CA 94720

² Structural Analyst, Arup, 560 Mission Street, San Francisco, CA 94105

³ Professor, Dept. of Civil and Environmental Engineering, UC, Berkeley, CA 94720

This paper examines the response of a single SCBF system as predicted using OpenSees with fiber-based elements and the general-purpose finite element software LS-DYNA (LSTC 2007) with shell elements. The comparison provides an overview of the similarity and the difference between such modeling approaches. In addition to considering differences between fiber and shell element models, results are also compared for models with and without the effects of low-cycle fatigue. The results reveal the strengths and weaknesses of different analytical tools and modeling assumptions.

Archetype Building

This paper is confined to an assessment of the seismic response of a single three-story tall SCBF building. As shown in Fig. 1, earthquake load resistance is provided by a single, one-bay wide SCBF located on each perimeter face of the building. It is assumed that the contributions of the gravity-load-only resisting frames to the lateral stiffness and strength of the structure are negligible.

The archetype building was designed (DASSE 2007) as a commercial office building (Occupancy Category II) for a location in downtown Los Angeles, CA. The provisions of ASCE 7-05 (2005) were followed in the design. The importance and redundancy factors were assumed to be unity. Table 1 lists some of the principal parameters used in the seismic design. The fundamental period estimated from the basic design code equation is 0.35 seconds, while the fundamental periods computed by eigenvalue analysis of the structural models used are approximately 0.5 second. More information on the design of the archetype building can be found in the reference (DASSE 2007).

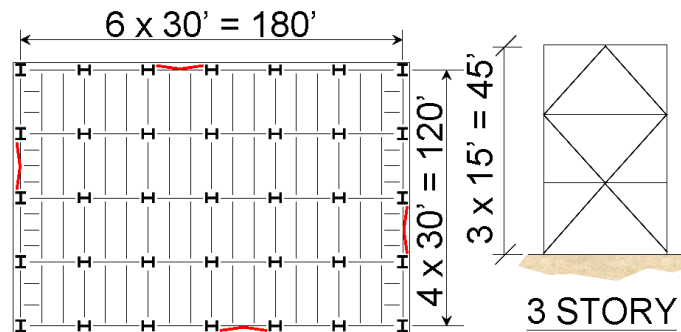


Figure 1. Archetype building floor plan and elevation.

Table 1. Design parameters of model building.

Code	ASCE 7-05
Short Period Spectral Acceleration, S_s	2.20g
1 sec. Period Spectral Acceleration, S_1	0.74g
R, Ω, C_d	6, 2, 5
Estimated Fundamental Period	0.35 sec.
Design Base Shear	0.24W

The structure was analyzed considering sixty ground motion records. These records were taken from the SAC ground motion ensembles developed consistent with 1997 NEHRP seismic hazard curves for Los Angeles (Somerville 1997). The sixty records represent three different hazard levels (2% probability of exceedence in 50 years, 10% in 50 years and 50% in 50 years). The median elastic spectral displacements corresponding to the fundamental period of the various models are shown in Table 2 for the three hazard levels.

Table 2. Median of $S_{d,Elastic}$ (inch).

Fundamental Period of Model	Hazard Level		
	50% in 50yrs	10% in 50yrs	2% in 50yrs
0.50 sec.	1.70	2.74	4.13

Numerical Models

Fiber-based models of the archetype structure were developed using OpenSees (McKenna 1997) and shell-based finite element models were developed using LS-DYNA (LSTC 2007). Modeling using the two software packages was as identical as possible. In both cases, only one braced bay was considered, subjected to vertical gravity dead loads and in-plane horizontal seismic excitations applied at the base. Half of the tributary reactive mass of the building was assigned to each frame, so that torsional response of the structure about a vertical axis was not considered. The gravity-load-only framing was idealized so it provided no structural strength or stiffness, but resulted in appropriate geometric nonlinearity effects. For the sake of clarity and simplicity in these comparisons, the vertical component of seismic excitation and the mechanical characteristics of the floor slabs were ignored.

OpenSees model

OpenSees models are designated 3BF2L and 3BF2LN, which employ fatigue material and non-fatigue material respectively. The columns in the SCBF bay are continuous and assumed fixed at their base as shown in Fig. 2. The beams are considered rigidly connected to the columns in both models. At connections with gusset plates, the behavior is very nearly fixed, even if such connections are not detailed as being fully restrained. The braces including the gusset plates in the ends were modeled with force-based nonlinear beam-column element. Fiber sections were used for the critical sections where yielding might occur. The beam and columns were modeled similarly to capture inelastic behavior. A corotational formulation was used to model member buckling while local buckling was not explicitly modeled. An empirical cycle counting method was used to simulate rupture due to low-cycle fatigue (Uriz and Mahin 2008). The vertical floor mass tributary to the braces intersecting a beam or column was included in the models. Earlier studies (Khatib et. al. 1988) showed that this vertical mass has a significant effect on dynamic response during brace buckling. P- Δ effects were represented using either one or two leaning columns. Each leaning column was constrained to have the same lateral displacement as the most adjacent column at a level in the braced bay. The axial and flexural stiffness of the columns are assumed to be large, but a pin was introduced at the bottom of the column in each story.

LS-DYNA model

The finite element models of the archetype structure were formulated in three dimensions using LS-DYNA as illustrated in Fig. 3. The analysis models explicitly simulate local buckling and evolution of damage due to low-cycle fatigue (Huang and Mahin 2008). To be consistent with the OpenSees models, lateral-torsional response of beams and lateral buckling of columns were neglected.

All components except the leaning columns were modeled as shell elements incorporating the damaged plasticity material model. No rigid elements are incorporated in the model. Similar to the OpenSees model, the vertical floor mass tributary to the braces and the dual pin-connected leaning column was modeled on each floor level to account for P- Δ effects. The beams in the gravity-only system were disregarded. A significant difference between the fiber and shell element models was that the beam-to-column connections away from gusset plates were modeled in LS-DYNA as welded shear tab connections, rather than as the moment connections modeled in OpenSees.

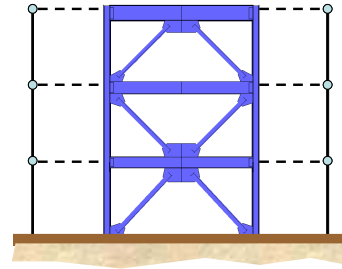
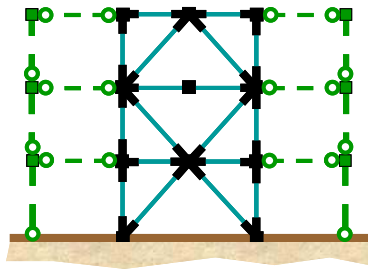


Figure 2. Sketch of basic OpenSEES model. Figure 3. Sketch of basic LS-DYNA model.

Individual Case Studies of Dynamic Response

Time histories of critical story drift and hysteretic loops for the frame roof displacement-base shear are examined in this section for Record LA32 (a simulated time history for a magnitude 7.1 earthquake on the Elysian Park fault). It is part of the ensemble scaled to be representative of hazard having a 2% in 50-year probability of exceedence.

Fig. 4 plots the story drift and brace axial deformation time histories at the first (bottom) story for record LA32. This ground motion causes the largest displacement responses in the model buildings. The bottom story suffered the largest story drifts for this (and most other) records, with the upper two stories remaining essentially elastic. For OpenSees models 3BF2L and 3BF2LN response to LA32 is characterized by a single very large story displacement excursion to about 14 to 20 inches at the first level. This corresponds to story drift ratios of around 8 to 11 percent. Permanent lateral roof displacements at the end of the record range from about 6 inches to 14 inches. This level of permanent lateral displacement may be difficult to repair. Results show that the story drifts in the fatigue sensitive model (3BF2L) increase significantly once fracture occurs and have larger residual deformations. The response of the LS-DYNA model is more similar to the OpenSees models without fatigue material (3BF2LN) due to the gradual increase of damage rather than the sudden rapture of elements characteristic of the OpenSees models.

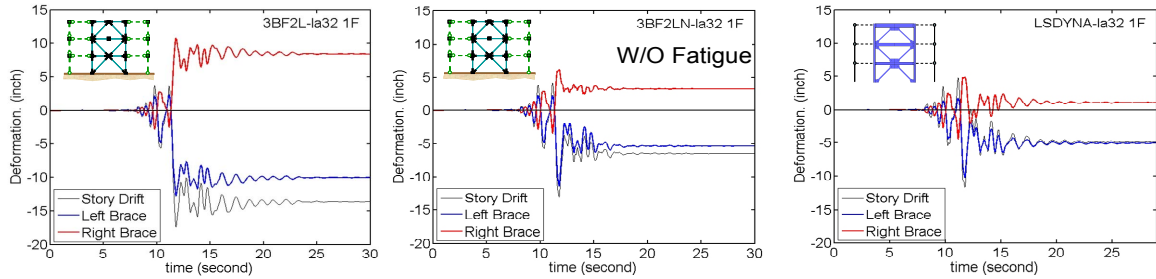


Figure 4. Time history of story drift and brace axial deformation in the ground story due to La32.

The brace axial deformation time histories show that the tension braces tend to have smaller axial deformation than the compression braces (comparing the absolute values). The slight sag of the beam in the brace-to-beam intersection causes this. Thus, the compression damage in the OpenSees models is greater than in tension as can be seen in Fig. 4.

The lateral drift – story shear hysteresis loops of each level are depicted in Fig. 5. Initially, all levels have about the same drift, but once lateral buckling occurs, drift tends to concentrate in the bottom story, with some smaller inelastic drifts in the second story. The third story remains nearly elastic throughout the response. The behavior of the OpenSees fiber model with material models including low-cycle fatigue is typified by fracture of the tension brace in the bottom level at a drift of about 10 inches (5.5% story drift). The cases with braces that fracture tend to displace further and remain offset, whereas the case without fracture considered tend to have smaller maximum drift, return towards the origin and have less residual displacement. The hysteretic strength and stiffness are reduced after the fracture.

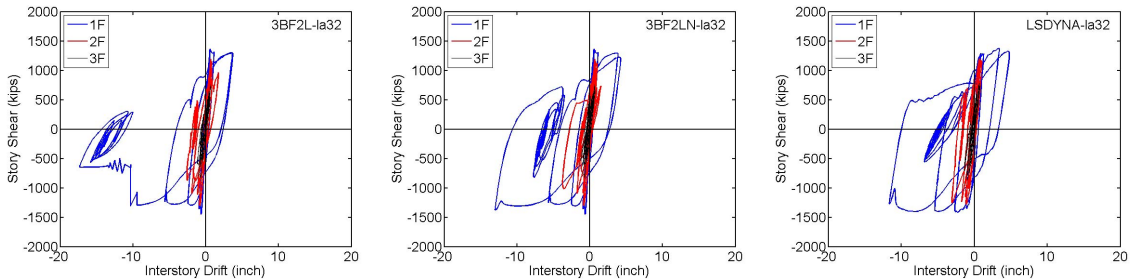


Figure 5. The relationship of story shear and story drift due to LA32.

The braces in the bottom story fracture during record LA32, but they may not fracture under different ground motions even if the fatigue sensitive material model is included. In such cases, the hysteresis loops maybe more similar to the models without fatigue, and the hysteresis behavior maybe more similar to the simulation in LS-DYNA model.

Statistical Evaluation of Predicted Story Drift Demands

Fig. 6 shows the relation of peak story drift ratio to $S_{d,Elastic}$ for each record used in the analysis. $S_{d,Elastic}$ is defined as the elastic spectral displacement for the record used in the analysis

at the fundamental period of the model being simulated. In these plots, IDRave is the peak roof displacement divided by the total height of the model building (which is thus the average story drift ratio); IDRmax is the maximum story drift ratio occurring at any of the three stories. The ratio of IDRmax/IDRave can be regarded as the index of the tendency of the system to form a soft story. The higher the ratio, the more concentrated the damage is in a single story.

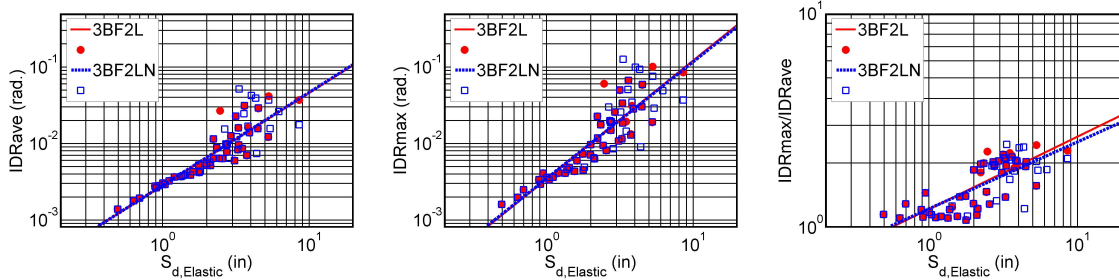


Figure 6. Comparison of Story Drift Ratios between fatigue model (3BF2L) and non-fatigue model (3BF2LN).

Linear regression analyses have been performed considering all of the results for a particular model to obtain relations of the lognormal form $\ln(\text{IDR}) = b + m \cdot \ln(S_{d,\text{Elastic}})$. The regression parameters are so similar that the differences of m and b between models are within 3%. While the trends are similar, there are several data points showing large inelastic demands when $S_{d,\text{Elastic}}$ becomes large. The case study, ground motion LA32, is among the cases producing demands larger than predicted by the regression relation. A nonlinear regression model may be more suitable for these structures to account for this increased response at large $S_{d,\text{Elastic}}$ values. Later, improved results obtained an intensity measure based on inelastic spectral displacement are presented.

Fig. 6 compares the effect of fatigue sensitive materials. Statistically, the results exhibit very limited difference. Although the case study presented of the response to the LA32 record indicated that responses of different models could differ significantly, regression curves based on response to many records are quite similar.

The median of maximum interstory drift ratios and residual interstory drift ratios corresponding to different hazard levels are listed in Table 3. These are determined from the trend lines identified in Fig. 6, the similar regression curve for residual IDR's, and the values of $S_{d,\text{Elastic}}$ in Table 2 corresponding to the hazard spectra for the site and the computed fundamental period of the structure. For the most severe hazard level (2% probability of exceedence in 50 years), the median expected maximum IDR values are about 3.0%. For the 10% in 50 years hazard level, the expected median maximum IDR are about 1.6%. For the story drift index at onset of brace buckling (about 0.3%), these maximum IDRs correspond to story drift ductilities of more than 10 and 5 for the 2% and 10% in 50-year hazard levels, respectively. The effect of fatigue sensitive materials is more important for the residual displacement than for the peak displacement. For the OpenSees model which employs the fatigue sensitive materials, the expected median maximum residual story drifts are about 1.4% and 0.3% for the 2% and 10% in 50-year hazard levels, respectively. The fracture of fibers in the braces reduces the restoring capacity of the frame and results in slightly larger residual drifts than those of the model without

incorporating the fatigue materials. These residual story drifts can be used to determine whether it is feasible or cost effective to repair a structure after an earthquake. However, further investigation is required for their application under PBEE framework in real practice.

Table 3. Median expected engineering demand parameters corresponding to different hazard levels based on elastic displacement spectra.

Model	IDRmax (% radian)			Res. IDR (%rad.)		
	50/50	10/50	2/50	50/50	10/50	2/50
3BF2L	0.75	1.65	3.03	0.05	0.32	1.39
3BF2LN	0.75	1.65	3.04	0.04	0.23	0.80
LSDYNA	0.66	1.51	2.88	0.03	0.18	0.79

It is interesting to note that for all the models, the expected median maximum story drift ratio at the 50% in 50-year hazard level exceeds the drift needed to cause buckling of a brace (about 0.3%). Thus, following an occasional earthquake for which it may be desired that no structural damage would occur that requires repair, it may be necessary to replace one or more braces, and repair nonstructural damage in adjacent elements.

For the application of performance-based design, a relation is developed from the regression analyses describing the probability that a value of IDRmax is exceeded for a given value of $S_{d,Elastic}$. In Fig. 7, fragility curves are presented for maximum story drifts ratios of 0.3% and 2.5%. These are simplified proxies for the initiation of brace buckling and the maximum drift accepted by standard code design methods for a Design Basis Event (ASCE 7-05).

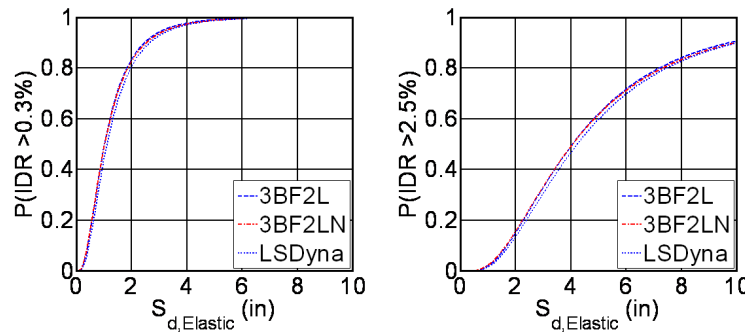


Figure 7. Probability of exceeding critical drifts for different models.

The probability that the maximum story drift ratio will exceed 0.3% and 2.5% for earthquakes with a given probability of exceedence can be obtained from Fig. 7. For a 2% in 50-year hazard level, both OpenSees models have more than 57% probability of developing maximum story drifts greater than 2.5%. For the 10% in 50-year hazard level, these probabilities drop to 33%. Considering the 50% in 50-year hazard level, the models have more than 80% probabilities of buckling a brace at one or more levels. This points out the need to consider the likely motion of the brace in the buckled configuration to minimize significant local nonstructural damage during service level events, and the possible need to replace braces following such events due to permanent lateral offsets.

Inelastic spectrum displacement as ground motion intensity measure

To investigate whether the substantial dispersion of the results plotted in Fig. 6 can be reduced, alternative ground motion intensity measures (IM) can be considered (e.g., Ruiz-Garcia and Miranda 2006). Below, results are shown for the case where an inelastic spectrum displacement is used as the ground motion intensity measure. The inelastic spectrum displacement is based on the first mode characteristics of the model building and generated from the software application BiSpec (Hachem 2005). The strength and stiffness properties of the equivalent single degree of freedom system are based on the static pushover analyses results using the procedure outline by Chopra (2006). A bilinear model is used to represent the hysteretic behavior of the structure. Inelastic displacements are computed for each of the 60 ground motions used in the study, and the peak displacements $S_{d,Inel}$ are used instead of $S_{d,Elastic}$ to plot the peak engineering demand parameters.

As can be seen in Fig. 8, the scatter of the results for peak IDR is significantly reduced compared to previously plotted cases using $S_{d,Elastic}$. To check the goodness of the fit, the R-square of the fit of the IDRmax- $S_{d,Inel}$ relation is shown in Table 4. The inelastic spectrum displacement substantially improves the dispersion of the IDRmax- $S_{d,Inel}$ relation, and the tendency of the IDR to exceed the regression curve for high intensity shaking is no longer apparent. It appears that this discrepancy may be thus associated with the “energy preserved” tendency that has been noted for single degree of freedom inelastic structures with relatively short periods (Chopra 2006). This is captured by the nonlinear analysis for the single degree of freedom systems used to obtain $S_{d,Inel}$. This may not be appropriate for systems having greater contributions of higher modes to response or for systems with longer periods.

Table 4. R-square of the fit of IDRmax and Sd relation for different models.

R-square	3BF2L	3BF2LN	LS-DYNA
IDRmax vs. $S_{d,Elastic}$ relation	0.8021	0.7473	0.7577
IDRmax vs. $S_{d,Inel}$ relation	0.9618	0.9728	0.9642

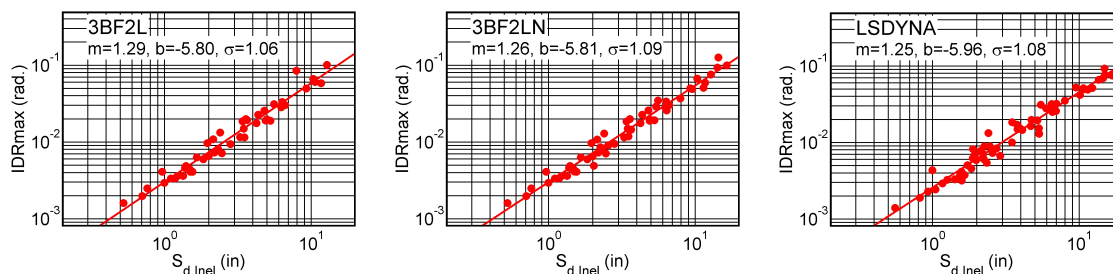


Figure 8. Relationship of Maximum Interstory Drift Ratio and inelastic spectrum displacement for different models.

A comparison of different models with intensity measures based on elastic and inelastic displacement spectra is shown in Fig. 9. The period of the LS-DYNA model is 0.52 second while that of OpenSees model is 0.5 second, so the values of S_d for the OpenSees and LS-DYNA

models are virtually the same. The difference in expected IDRmax values for OpenSees model and LS-DYNA models is less than 10%.

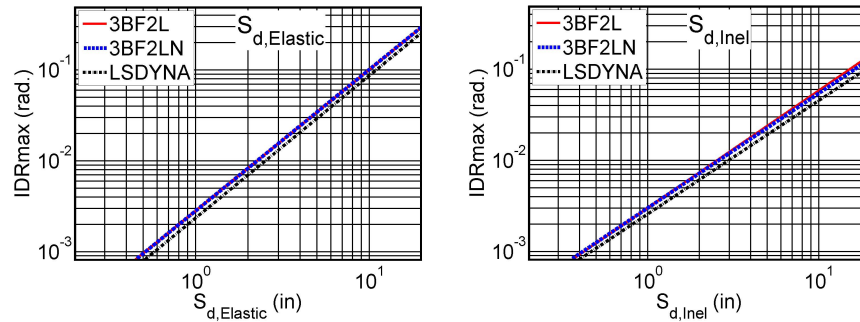


Figure 9. Trend lines of IDRmax and S_d for different models.

Conclusions

Analytical studies of a three-story tall SCBF building were conducted using fiber-based models from the computational platform OpenSees and using shell elements from the finite element software program LS-DYNA. Analytical results of each model were interpreted and compared in terms of a case study under a single earthquake record and a probabilistic analysis of results using sixty ground motions representative of different hazard levels.

Results for the short-period SCBF system demonstrate that using inelastic spectral displacements instead of ones based on elastic analysis substantially reduce dispersion of the results especially for large intensity events.

Comparison of inelastic behavior predicted by different models for individual ground motion records shows that the difference between beam-element and shell element models can be significant. For the ground motions used in this study, shell-element models in LS-DYNA predicted smaller maximum story drift and residual story drift. Moreover, the ultimate failure modes may differ significantly for the two approaches. On the other hand, from a statistical perspective (when inelastic spectrum displacement is used as the intensity measure), the difference between OpenSees beam-element model and LS-DYNA shell-element model results is less than the dispersion for different ground motions by the same model. This shows for the case considered herein that if inelastic spectrum displacements are used to predict the structural responses, corresponding inelastic properties can be obtained from analysis using beam- or shell-element model, resulting in equally accurate prediction.

Acknowledgments

This work is an extension of previous work by Dr. Patxi Uriz. His assistance in developing the numerical models and providing advice is greatly appreciated. Rafael Sabelli designed the SCBF structures considered herein. His efforts to design the archetype structure and provide advice related to interpretation of code requirements contributed to the success of this effort. The assistance of Andreas Schellenberg and Silvia Mazzoni in developing the OpenSees

models is gratefully acknowledged.

This material is based upon work supported in part by the National Science Foundation under Grant No. CMS-0600625 -- Robust Performance-based Design of Concentrically Braced Steel Frame Buildings, and Grant No. 0619161 -- International Hybrid Simulation of Tomorrow's Braced Frame Systems, as well as the Byron and Elvira Nishkian Professorship in Structural Engineering. Any opinions, findings, and conclusions or recommendations expressed in this material are those of the authors and do not necessarily reflect the views of the National Science Foundation or the University of California.

References

- ASCE 7 (2005), *ASCE Standard Minimum Design Loads for Buildings and Other Structures*, ASCE 7-05, American Society of Civil Engineers, Reston, VA.
- Chopra, A. (2006) *Dynamics of Structures*, Prentice Hall, New York.
- DASSE (2007), *Cost Advantages of Buckling Restrained Braced Frame Buildings*, DASSE Design Inc.
- Hachem, M. (2008). "BiSpec 1.61" Berkeley, CA,
<http://www.ce.berkeley.edu/~hachem/bispec/index.html>.
- Huang, Y., and Mahin, S. A. (2008). "Evaluation of Steel Structure Deterioration with Cyclic Damaged Plasticity." *Proceedings, 14th World Conference on Earthquake Engineering*, October 12-17, 2008, Beijing, China.
- Khatib, I., Mahin, S. and Pister, K. (1988), *Seismic behavior of concentrically braced steel frames*, UCB/EERC-88/01, Earthquake Engineering Research Center, University of California, Berkeley, 1988-01
- LSTC (2007). *LS-DYNA Keyword User's Manual*, Livermore Software Technology Corporation, CA, US.
- McKenna, F. (1997). *Object Oriented Finite Element Programming: Frameworks for Analysis, Algorithms and Parallel Computing*, University of California, Berkeley, Berkeley, CA 94720.
- NEHRP (1997), *Recommended Provisions for the Development of Seismic Regulations for New Buildings (and other Structures)*, Building Seismic Safety Council, Washington, D.C.
- Ruiz-Garcia, J. and Miranda, E. (2006). "Evaluation of residual drift demands in regular multi-storey frames for performance-based seismic assessment," *Earthquake Engineering & Structural Dynamics*. Vol. 35, no. 13, pp. 1609-1629. 10 Nov. 2006
- Somerville, P. G. (1997). Development of ground motion time histories for phase 2 of the FEMA /SAC Steel Project. *SAC BD/97-04*, SAC Steel Joint Venture, Sacramento, California.
- Uriz, P and Mahin, S. (2008), *Towards earthquake resistant design of concentrically braced steel structures*, Report PEER 2008/08, Pacific Earthquake Engineering Research Center, University of California, Berkeley, CA.